SC5162.2SA

Copy No. _____

TEMPERATURE-COMPENSATED PIEZOELECTRIC MATERIALS

Semi-Annual Report No. 1 for the Period
June 6, 1978 through November 30, 1978

January, 1979

ARPA Order No.	3570
Program Code:	8D10
Name of Contractor:	Rockwell International
Effective Date of Contract:	May 15, 1978
Contract Expiration Date:	May 14, 1980
Amount of Contract Dollars:	$372,101
Contract Number:	F49620-78-C-0093
Principal Investigators:	Dr. R. R. Neurgaonkar (805) 498-4545, X-109 Professor L. E. Cross Pennsylvania State University (814) 865-1181
Program Manager:	Dr. E. J. Staples (805) 498-4545, X-202

Sponsored by

Advanced Research Projects Agency (DOD)
ARPA Order No. 3570
Monitored by AFOSR under Contract No. F49620-78-C-0093

Rockwell International
Science Center

Unclassified

SECURITY CLASSIFICATION OF THIS PAGE (When Data Entered)

REPORT DOCUMENTATION PAGE	READ INSTRUCTIONS BEFORE COMPLETING FORM
1. REPORT NUMBER	2. GOVT ACCESSION NO. AD-A139 279 / 3. RECIPIENT'S CATALOG NUMBER
4. TITLE (and Subtitle) Temperature-Compensated Piezoelectric Materials	5. TYPE OF REPORT & PERIOD COVERED Semi-Annual 6-6-78 thru 11-30-78
	6. PERFORMING ORG. REPORT NUMBER SC5162.2SA
7. AUTHOR(s) R. R. Neurgaonkar and L. E. Cross	8. CONTRACT OR GRANT NUMBER(s) F49260-78-C-0093
9. PERFORMING ORGANIZATION NAME AND ADDRESS Science Center, Rockwell International Thousand Oaks, CA 91360	10. PROGRAM ELEMENT, PROJECT, TASK AREA & WORK UNIT NUMBERS ARPA Order No. 3570
11. CONTROLLING OFFICE NAME AND ADDRESS Air Force Office of Scientific Research Bolling Air Force Base Washington, DC 20332	12. REPORT DATE January, 1979
	13. NUMBER OF PAGES 27
14. MONITORING AGENCY NAME & ADDRESS (if different from Controlling Office)	15. SECURITY CLASS. (of this report) Unclassified
	15a. DECLASSIFICATION DOWNGRADING SCHEDULE

16. DISTRIBUTION STATEMENT (of this Report)

Approved for release; distribution unlimited

17. DISTRIBUTION STATEMENT (of the abstract entered in Block 20, if different from Report)

18. SUPPLEMENTARY NOTES

19. KEY WORDS (Continue on reverse side if necessary and identify by block number)

Temperature-compensated piezoelectric materials
Ferroelectric and ferroelastic materials
Liquid phase epitaxy in tungsten bronzes
Tungsten-bronze crystal family

20. ABSTRACT (Continue on reverse side if necessary and identify by block number)

During the first and second quarters of the present contract, an initial literature survey of all known tungsten-bronze compounds was completed. Preliminary formulation of the Gibb's energy function for ferroic materials to describe the phase transitions has been accomplished. Apparatus to perform LPE growth of tungsten-bronzes has been constructed and several suitable flux systems for the growth of strontium-barium-niobate (SBN) films have been found. From an analysis of the chemistry of SBN, several new compounds have been identified and may be readily obtained by element substitutions within the SBN structure.

DD FORM 1 JAN 73 1473 EDITION OF 1 NOV 65 IS OBSOLETE

Unclassified

TABLE OF CONTENTS

LIST OF TABLES

1.0 TECHNICAL REPORT SUMMARY

1.1 Technical Problem

The technical problem is to determine why known ferroelectric and ferroelastic materials are temperature-compensated and to predict such occurences. Knowledge from such a determination will be used to grow and characterize suitable crystals from the tungsten-bronze crystal family using liquid phase epitaxy techniques. The end goal is to provide high-coupling, temperature-compensated materials for minimum shift keyed (msk) surface wave filters.

1.2 General Methodology

A literature survey of the known tungsten-bronze compounds is providing the data necessary for the development of a phenomenological model based on Gibb's energy function to explain the nature of temperature compensation in these types of crystals. Experimentally, films of tungsten-bronze crystals are to be grown via liquid phase epitaxy. Material characterization will provide experimental confirmation or indicate needed modifications to the theoretical model.

1.3 Technical Results

During the first and second quarters of the present contract, an initial literature survey of all known tungsten-bronze compounds was completed. Preliminary formulation of the Gibb's energy function for ferroic materials to describe the phase transitions has been accomplished. Apparatus to perform LPE growth of tungsten-bronzes has been constructed and several suitable flux systems for the growth of strontium-barium-niobate (SBN) films have been found. From an analysis of the chemistry of SBN, several new compounds have

been identified and may be readily obtained by element substitutions within the SBN structure.

1.4 Implications for Further Research

During the third and fourth quarters of this contract, we will apply the phenomenological model to the data available for SBN as well as other tungsten-bronze ferroelectrics. Crystal growth of SBN will be performed and the elastic, piezoelectric and dielectric properties of this material measured.

1.5 Special Comments

At this time a limited supply of bulk SBN crystals has been obtained from the University of Tokyo, Honeywell Research Laboratories, and Stanford University. These materials are being used for bulk crystal characterization studies and also as seed crystals for our own crystal growth program. We expect a larger supply of SBN substrates for LPE growth to result from our IR&D program.

2.0 RESEARCH RESULTS

2.1 Literature Survey

The initial digest of the literature on the ferroelectric bronze family of materials has amply confirmed the expected variety in the chemistry of the bronzes. With the considerable flexibility of the tetragonal bronze prototype it is difficult to separate compounds from solid solutions, and a limited range of mixed oxide off-stoichiometry is to be expected in all the compounds listed. For the purpose of these studies, we have chosen to list as separate compounds all chemically distinct compositions $A_xB_yC_z...O_{30}$ where x,y,z... are whole numbers.

So far, using the data compilation by Landolt-Bornstein (Vol. 3 and Vol. 9), the "Digest of the Literature on Dielectrics," and the ORNL literature guides as starting points, 80 separate ferroelectric bronze compounds have been identified. Original literature has been traced for 68 of these compounds listed in Table I.

The purpose of the present data compilation is two-fold:

1. To provide accessible structural information so that the range of choices for host and epitaxial film compositions can be rapidly evaluated.
2. For the phenomenological analysis, and its extension to solid solution systems, the data base in properties which have been measured on well-characterized single crystals of the end member compositions is fundamentally important. With the escalating size and complexity of the listing of the bronze structure compounds, it was decided that

Table Ia. Tungsten-Bronze Compounds

Compounds	Available Data[2]											
	STR[1]	T_c (°C)	Lattice Constants			Therm α_{ij}	ε_{ij}	P_s	Pyro P_i	Piezo d_{ijk}	Elastic e_{ij}, s_{ij}
			a_o	b_o	c_o						
$PbNb_2O_6$	O	560	17.51	17.81	7.73	*	T				
$Ba_2NaNb_5O_{15}$	O	560	17.591	17.625	7.992	*	T			T	T
$Pb_2NaNb_5O_{15}$	O	531	17.606	17.928	3.856						
$Pb_2KNb_5O_{15}$	O	460	17.78	18.05	3.917		T			*	*
$K_3Li_2Nb_5O_{15}$	T	420	12.560		4.039		T				
$Ba_5NaNb_9TiO_{30}$	T	414	12.50		4.00		T	T			
$Ba_4Bi_2Fe_2Nb_8O_{30}$	T	400	12.53		3.960						
$Ba_2KNb_5O_{15}$	T	373	12.55		4.019		*				
$K_2BiNb_5O_{15}$	O	350	17.75	17.90	7.84		T				
$Ba_2Na_3YNb_{10}O_{30}$	T	306	12.41		3.924						
$Ba_5KNb_9TiO_{30}$	T	290	12.52		4.01		T				
$K_2TbNb_5O_{15}$	T	280	12.440		3.910						
$K_2DyNb_5O_{15}$	T	280	12.431		3.903						
$BaSrKNb_5O_{15}$	T	278	12.520		3.975						

[1] T = Tetragonal, O = Orthorhombic

[2] * = Data reported; T = Data reported as a function of temperature
x = Data reported as a function of composition

Table Ib. Tungsten-Bronze Compounds

Compounds	Available Data[2]										
	STR[1]	T_c (°C)	Lattice Constants			Therm α_{ij}	ϵ_{ij}	P_s	Pyro P_i	Piezo d_{ijk}	Elastic e_{ij}, s_{ij}
			a_o	b_o	c_o						
$BaSrNaNb_5O_{15}$	T	274	12.443		3.945			x			
$Sr_2NaNb_5O_{15}$	T	266					T				
$BaCaKNb_5O_{15}$	T	266	12.442		3.954						
$PbTa_2O_6$	O	265	17.68	17.72	7.754	*	T				
$K_2GdNb_5O_{15}$	T	250	12.450		3.912						
$Ba_2Na_2YNb_{10}O_{30}$	T	220	12.400		3.900						
$Ba_2Na_3DyNb_{10}O_{30}$	T	220	12.405		3.893						
$K_2EuNb_5O_{15}$	T	205	12.457		3.914						
$Ba_4Sr_2Nb_8Ti_2O_{30}$	T	200	12.44		3.94		*				
$K_2SmNb_5O_{15}$	T	195	12.474		3.917						
$Sr_4Ca_2Nb_8Ti_2O_{30}$	T	170	12.27		3.86		*				
$Ba_2Na_3CdNb_{10}O_{30}$	T	170	12.417		3.895						
$K_2NdNb_5O_{15}$	T	160	12.497		3.924						
$Sr_5NaNb_9TiO_{30}$	T	157	12.36		3.80						

[1] T = Tetragonal, O = Orthorhombic

[2] * = Data reported; T = Data reported as a function of temperature
x = Data reported as a function of composition

Table Ic. Tungsten-Bronze Compounds

Compounds	Available Data[2]										
	STR[1]	T_c (°C)	Lattice Constants			Therm α_{ij}	ε_{ij}	P_s	Pyro P_i	Piezo d_{ijk}	Elastic c_{ij}, s_{ij}
			a_o	b_o	c_o						
$Sr_2KNb_5O_{15}$	T	156	12.47		3.942		T	*			
$Ba_2Na_3EuNb_{10}O_{30}$	T	155	12.429		3.902						
$Ba_3NaYNb_{10}O_{30}$	T	145	12.423		3.933						
$Sr_2RbNb_5O_{10}$	T	139	12.51		3.949		*				
$Sr_6Nb_8Ti_2O_{30}$	T	130	12.36		3.89		T				
$Ba_3Gd_2Fe_2Nb_8O_{30}$	T	130									
$Ba_4Sm_2Fe_2Nb_8O_{30}$	T	130	12.46		3.926			*			
$BaSrNb_4O_{12}$	T	125	12.40		3.930	*	T,x	T	*	*	*
$Sr_5KNb_9TiO_{30}$	T	118	12.38		3.90		T				
$Sr_2KTa_5O_{15}$	O	110	17.550	17.660	3.890						
$Ba_4Ca_2Nb_8Ti_2O_{30}$	T	80	12.37		3.92		*				
$Ba_3NaGdNb_{10}O_{30}$	T	20	12.449		3.394						
$K_3Li_2Ta_5O_{15}$	O	7	17.78	17.83	3.931						
$Ba_2Na_3LaNb_{10}O_{30}$	T	-25	12.460		3.955						

[1] T = Tetragonal, O = Orthorhombic

[2] * = Data reported; T = Data reported as a function of temperature
x = Data reported as a function of composition

Table Id. Tungsten-Bronze Compounds

Compounds	Available Data[2]										
	STR[1]	T_c (°C)	Lattice Constants			Therm α_{ij}	ϵ_{ij}	P_s	Pyro P_i	Piezo d_{ijk}	Elastic c_{ij}, s_{ij}
			a_o	b_o	c_o						
$Ba_3NaLaNb_{10}O_{30}$	T	- 50	12.475		3.950						
$K_2LaNb_5O_{15}$	T	- 90	12.58		3.93						
$Rb_2LaNb_5O_{15}$	T	-120			3.945						
$BaNa_2Nb_5O_{14}F$	T		12.369		3.928						
$SrNb_2O_6$	T		17.720		7.760						
$BaNa_2La_2Nb_{10}O_{30}$	T		12.475		3.904						
$K_2CeNb_5O_{15}$	T		12.545		3.913						
$K_2PrNb_5O_{15}$	T		12.530		3.918						
$K_2HoNb_5O_{15}$	T		12.426		3.899						
$K_2YNb_5O_{15}$	T		12.424		3.901						
$Ba_2Nd_4Fe_3Nb_7O_{30}$	T		12.48		3.939		*				
$Ba_2Sm_4Fe_3Nb_7O_{30}$	T		12.46		3.93		*				
$Pb_2Nd_4Fe_3Nb_7O_{30}$	T		12.43		3.92		*				
$Bi_2Nd_4Fe_4Nb_6O_{30}$	T		12.54		3.86		*				

[1] T = Tetragonal, O = Orthorhombic

[2] * = Data reported; T = Data reported as a function of temperature
x = Data reported as a function of composition

translating and storing the data in computer format would be worthwhile. For the small extra effort required to put the data into this form, it is now possible to re-tabulate at will, sorting according to any particular physical parameter. In the tabulation given in Table I, for example, the compounds have been ordered in descending ferroelectric transition temperatures (T_C).

A second advantage of using the computer for this function is the availability of a number of excellent graphics packages for the computer system. Further, since we shall be running much of the computation for the phenomenological analysis on this system, which is hard-wire interfaced with a larger system, appropriate storage techniques, handling, and processing of the property data should be greatly facilitated.

In the present phase, most of the available compound bronzes have been identified. The property information is now being taken from the original papers and cross-checked with subsequent studies wherever possible. Indication of this build-up is given in Table I.

The problem of handling the data for the many possible solid solutions in the bronze systems is our major concern in the first half of this study phase. Listings for two-component solid solutions are being made up in the form shown in Table II. Unfortunately, much of the original data are for ceramic (polycrystal) systems so that tensorial constants for the elastic, piezoelectric, and dielectric data are, as we expected, rather scarce. The major trends in dimensions, phase stability and Curie temperature are, however, available as starting points for the phenomenological analysis.

Table II. Strontium-Barium-Niobate Solvents

System	Melting Temp. (°C-Flux)	Eutectic Temp. (°C)	Phases Present	Remarks
V_2O_5-$Sr_{1-x}Ba_xNb_2O_6$	690	--	TB + Unknown	Not Suitable
WO_3-$Sr_{1-x}Ba_xNb_2O_6$	1420	--	TB + Unknown	Not Suitable
KVO_3-$Sr_{1-x}Ba_xNb_2O_6$	520	~ 490	TB + KVO_3	Useful--Long Crystallization Range
$NaVO_3$-$Sr_{1-x}Ba_xNb_2O_6$	630	~ 560	TB + Unknown	In Progress
BaV_2O_6-$Sr_{1-x}Ba_xNb_2O_6$	700	--	TB + BaV_2O_6	Useful--Long Crystallization Range
Na_2WO_4-$Sr_{1-x}Ba_xNb_2O_6$	700	~ 650	TB + Unknown	In Progress
K_2WO_4-$Sr_{1-x}Ba_xNb_2O_6$	920	--	TB + K_2WO_4	In Progress
$LiVO_3$-$Sr_{1-x}Ba_xNb_2O_6$	616	--	$LiNbO_3$ + Unknown	Not Suitable
Li_2WO_4-$Sr_{1-x}Ba_xNb_2O_6$	700	--	$LiNbO_3$ + Unknown	Not Suitable

TB = Tetragonal tungsten-bronze type structure

2.2 Theoretical Treatment of Tungsten-Bronze Ferroelectrics

The present approach to a phenomenological description of the elasto-electric behavior of the tungsten-bronze family of ferroelectrics is predicted on the assumption that if a material has a direction of propagation for a bulk wave in which the delay time is independent of temperature, it will be of interest also for surface acoustic wave devices (SAW) and will have a high probability of also having temperature-compensated directions for SAW. This is especially true if the bulk shear modulus is temperature-compensated.

The conditions which dictate the temperature coefficient of delay for a bulk wave have been given as

$$\frac{1}{\tau}\left(\frac{\partial\tau}{\partial T}\right)_P = \alpha_s - \frac{1}{2}\alpha_v - \frac{1}{2}\frac{1}{\bar{C}}\left(\frac{d\bar{C}}{dT}\right)_P \tag{1}$$

where α_s is the linear thermal expansion coefficient in the direction of propagation, α_v is the volume expansion coefficient, and

$$\bar{C}_{ijk\ell} = C^E_{ihk\ell} + \frac{d_{pij}d_{qk\ell}N_pN_q}{\epsilon^x_{rs}N_rN_s} \tag{2}$$

is the effective elastic constant tensor for the piezoelectric. The first term in Eq. (2) is the adiabatic elastic constant at constant electric field. The second term is the piezoelectric stiffening term which depends not only on the piezoelectric tensor, but also on the dielectric permittivity tensor and the direction cosines of the wave vector K (the N_{js}).

The elastic constant which appears in (2) can be for a general direction, thus for an orthorhombic bronze the temperature coefficient of delay is controlled by nine elastic, five piezoelectric, and three dielectric constants

and their temperature derivatives, and three independent thermal expansion coefficients. While in the tetragonal bronze the situation is only slightly easier with eight elastic, three piezoelectric, two dielectric constants, and two independent expansion parameters.

It would indeed be a daunting task to measure up all of these constants and derivatives in the full family of bronze composition which have been identified. On the other hand, because of the complexity of the bronze structure, it is not yet possible to go back to first principles and derive from atomistic models values of the parameters and derivatives which would be meaningful. What is possible, however, is the separation of those features of the behavior which originate in the ferroelectric and ferroelastic properties of the bronze from those which are characteristic of the higher symmetry tetragonal prototypic state.

The procedure for such a separation is to set up a phenomenological elastic Gibbs function for the prototype, which contains the appropriate higher order terms which are symmetry-permitted and which are required to stabilize the known ferroelectric and ferroelastic transitions.

Since the symmetry of the tetragonal prototype is common to all bronzes, the form of the functions does not change throughout the whole family. The magnitudes of the parameters and their temperature coefficients will, of course, change, but experience with other simpler systems suggests that the major temperature dependence is confined to only a few characteristic parameters. Identification of the parameters which are responsible for the phase changes into the different ferroic phases is an important first task in the phenomenological description.

Formally, the Gibbs function may be split into three components.[1]

$$\Delta G = \Phi_1(\eta\rho) + \Phi_2(XP) + \Phi_3(XP\eta\rho)$$

Φ_1 is a function of the independent components η and ρ of the order parameter which characterizes the improper ferroelectric phase.

Φ_2 contains the contributions related to the elastic, dielectric, and elasto-electric (electrostrictive) energies of the crystal.

Φ_3 represents the coupling between the order parameters for the ferroelasticity and the stress and polarization components.

The function Φ_1 must contain up to sixth-order invariants to describe the thermodynamically first-order nature of the ferrcelastic phase change, i.e.,

$$\Phi_1 = \frac{1}{2}\alpha(\eta^2 + \rho^2) + \frac{1}{4}\beta_1(\eta^4 + \rho^4) + \frac{1}{2}\beta_2\eta^2\rho^2 + \frac{1}{6}\gamma_1(\eta^6 + \rho^6)$$
$$+ \frac{1}{2}\gamma_2\eta^2\rho^2(\eta^2 + \rho^2) \qquad (3)$$

The function Φ_2 must also be expanded to include the first permitted sixth-order terms to describe thermodynamically the first-order proper ferroelastic phase changes,

$$\Phi_2 = \alpha_1^x (P_1^2 + P_2^2) + \alpha_3^x P_3^2 + \alpha_{11}^x (P_1^4 + P_2^4) + \alpha_{33}^x P_3^4$$
$$+ \alpha_{13}(P_1^2 P_3^2 + P_2^2 P_3^2) + \alpha_{12}^x (P_1^2 P_2^2 + \alpha_{333}^x P_3^6$$
$$+ \alpha_{111}^x (P_1^6 + P_2^6) - \frac{1}{2} s_{11}^P (X_1^2 + X_2^2) - s_{12}^P X_1 X_2$$
$$- s_{13}^P (X_1 + X_2) X_3 - \frac{1}{2} s_{33}^P X_3^2 - \frac{1}{4} s_{44}^P (X_4^2 + X_5^2)$$
$$+ Q_{13}(P_1^2 X_3 + P_2^2 X_3) + Q_{31}(P_3^2 X_1 + P_2^2 X_2)$$
$$+ Q_{33} P_3^2 X_3 + Q_{44}(P_2 P_3 X_4 + P_1 P_x X_5)$$
$$+ Q_{66} P_1 P_2 X_6$$

while the lowest order interaction terms give

$$\Phi_3 = \theta_1 [X_1 + X_2][\eta^2 + \rho^2] + \theta_2 X_3 [\eta^2 + \rho^2]$$
$$+ \rho_1 [P_1^2 + P_2^2][\eta^2 + \rho^2] + \rho_2 P_3^2 [\eta^2 + \rho^2]$$
$$+ \nu_1 [X_1 - X_2][\eta^2 - \rho^2] + \nu_2 X_6 \eta\rho$$

At any temperature the stable or metastable states of the bronze crystal are given by

$$\frac{\partial \Delta G}{\partial \eta} = \frac{\partial \Delta G}{\partial \rho} = 0 \qquad \frac{\partial^2 \Delta G}{\partial \eta^2} = \frac{\partial^2 \Delta G}{\partial \rho} \geqslant 0$$

$$\frac{\partial^2 \Delta G}{\partial \eta^2} = \frac{\partial^2 \Delta G}{\partial \rho^2} > \left(\frac{\partial^2 \Delta G}{\partial \eta \partial \rho}\right)$$

$$\frac{\partial \Delta G}{\partial X_i} = \frac{\partial \Delta G}{\partial P_j} = 0$$

The coefficients which are strongly temperature-dependent and which dominate the balance of phases are

$$\alpha_1^x = \alpha_{1(o)}^x (T - \theta_1)$$

$$\alpha_3^x = \alpha_{3(o)}^x (T - \theta_2)$$

and

$$\alpha = \alpha_o (T - \theta_3)$$

If $\theta_1 < \theta_2$, and certain other conditions are satisfied on the higher order terms, the prototypic phase will transform first on cooling to an orthorhombic ferroelectric phase (mm2). For the condition $\theta_2 < \theta_1$ the transition will be into a tetragonal simple proper ferroelectric phase.

The coefficient θ_3 determines the temperature of the onset of improper ferroelastic phases.

The procedure which we are following involves the following steps:

1. From the dielectric constant, data for a wide range of bronze crystals to determine the magnitudes of $\alpha^{x}_{1(o)}$ and of $\alpha^{x}_{3(o)}$.
2. Using the polarization as a function of temperature to obtain values of the α_{ij} and α_{ijk}.
3. From the lattice constant measurement as a function of temperature to extract values for the spontaneous strains, then using the experimental and calculated P_1P_3 values to derive values for the electrostriction parameters Q_{11}, Q_{12}.
4. Wherever data are available, to calculate from the known Q and P values the piezoelectric constants and their temperature dependence.
5. To compute values of the s^{E}_{ij} from s^{P}_{ij} and the known Q and P values.

The basic objective of the approach is to sort out by the phenomenological method the prototypic lattice behavior from the total response which contains major contributions from the ferroelectric and improper ferroelastic instabilities.

Based on similar studies in the complex perovskites, the expectation is that there will be a very slow regular mutation in the parameters of the prototype, with only a limited range of values encompassing the whole field of stable compositions, and that the major "tuning" of the properties which is required for the particular device can be accomplished by the major manipulation of the ferroic transition temperatures and relative stabilities which can be embraced.

2.3 Crystal Chemistry and LPE Growth Techniques

A specific task of this contract is to establish techniques and construct suitable apparatus for liquid phase epitaxial (LPE) growth of selected materials identified in the above literature survey. During the first six months an LPE furnace, described in section 2.3.1, and its associated controls was constructed. As a result of the above literature survey and other considerations, it was decided the first member of the tungsten-bronze family to be studied would be strontium-barium-niobate (SBN or $Sr_{1-x}Ba_xNb_2O_6$). Flux systems suitable for the LPE growth of SBN are described in section 2.3 2. The compositional range, X, for SBN is exceptionally large, 0.25 to 0.75. The crystal chemistry of new tungsten-bronze solid-solutions that might be expected from element substitutions is discussed in section 2.3.3.

2.3.1 LPE Growth Apparatus

During the first part of this investigation, the LPE growth apparatus shown in Fig. 1 was constructed. The basic furnace consisted of a vertical platinum-wound resistance furnace capable of reaching 1500°C. It has an overall length of 20 inches with 2-1/2 inches internal diameter and external shunts at 2-inch intervals for adjusting the temperature profile. The temperature control system consists of an SCR power supply, high-stability supply controller (±0.2°C), and a temperature ramp generator for linearly varying the growth temperature up or down from 0.1 to 10°C/minute. Growth temperature is carefully monitored by placing two 90%-10% Rh-Pt thermocouples, one inside and the other outside the melt. The system also contains a substrate preheating furnace, 600-700°C, located

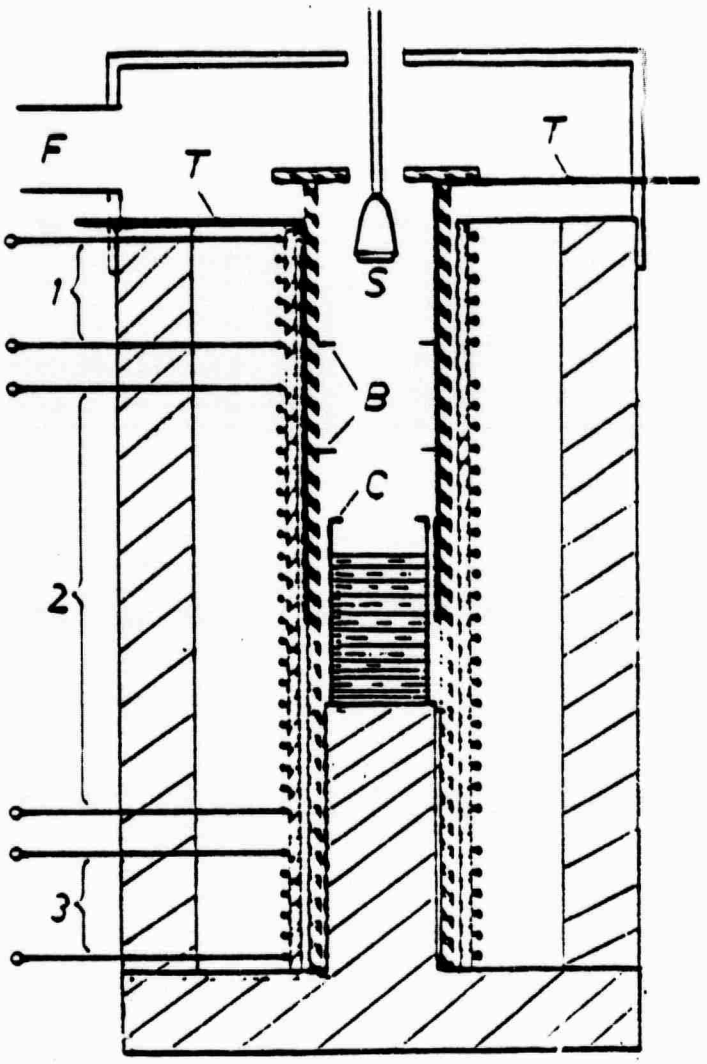

Fig. 1 Diagram of furnace for liquid phase epitaxy.

above the growth chamber, which isolates the substrate from any undesirable vapor during a preheating period. A lead-screw drive is used to lower or raise the substrate assembly holder through a predetermined distance from the top of the furnace to the appropriate immersion depth in the melt. This system is capable of traveling as slow as one inch per 20 minutes up or down, and rotating at 0.1 to 10 rps.

2.3.2 Tungsten-Bronze Solvents

In order to grow films by LPE, a suitable solvent flux must be found. THe following information is being studied:

1. Liquidus temperature as a function of composition.
2. Crystallization range of the phase to be crystallized and its stability at elevated temperature.
3. Viscocity as a function of composition and growth temperature.
4. Density as a function of composition and growth temperature.

In order to grow high-quality films, these parameters must be known. Since the present systems contain five or more components, the determination of a complete phase diagram in such a situation is impractical. As described by Roy and White,[2] such systems can be treated as a pseudo-binary system with the phase to be crystallized as one component (solute) and the flux (solvent) as the other. Using this concept, several flux-systems have been investigated for tungsten-bronze crystals. In particular, our goal was to crystallize the tungsten-bronze phase having the composition $Sr_{1-x}Ba_xNb_2O_6$. Table II documents the melting temperature, eutectic temperature and crystallization range for the flux systems thus far studied.

Our initial results indicated the oxides of V_2O_5 and WO_4 were very volatile when incorporated in flux systems. Their use has been discontinued and the alkali or alkaline earth vanadates and tungstates are now being used to determine the crystallization range of $Sr_{1-x}Ba_xNb_2O_6$. The $LiVO_3$, K_2WO_4 and Li_2WO_4 fluxes are relatively well known and have been used by ourselves as well as others to grow $LiNbO_3$ films.[3-5]

The results of our experiments indicate that $Sr_{1-x}Ba_xNb_2O_6$ can easily be crystallized as a stable phase from the systems KVO_3-$Sr_{1-x}Ba_xNb_2O_6$, $NaVO_3$-$Sr_{1-x}Ba_xNb_2O_6$, and BaV_2O_6-$Sr_{1-x}Ba_xNb_2O_6$. The X-ray powder diffraction technique has been used to determine the existence of the desired composition as well as to warn of the presence of undesirable compounds such as $Ba_2KNb_5O_{15}$, $Sr_2KNb_2O_{15}$, and $Ba_2NaNb_5O_{15}$ which also have the tungsten-bronze structure. A careful determination of the lattice constants of these phases is in progress and will provide a needed standard against which to compare thin films grown by LPE. Experiments with the flux BaV_2O_6-S_{1-x} $Ba_xNb_2O_6$ indicate that the tungsten-bronze phase of SBN is stable over much of the $BaNb_2O_6$ and $SrNb_2O_6$ phases. Since $BaNb_2O_6$ and $SrNb_2O_6$ belong to a different structural family, it appears possible to control the Sr:Ba ratio in the $Sr_{1-x}Ba_xNb_2O_6$ system through the BaV_2O_6 flux.

The remaining two flux systems, $LiVO_3$-$Sr_{1-x}Ba_xNb_2O_6$ and Li_2WO_4-$Sr_{1-x}Ba_xNb_2O_6$ did not produce a stable composition of SBN until at least 70 mole % of $Sr_{1-x}Ba_xNb_2O_6$, and would require a dipping temperature of at least 1200°C. $LiNbO_3$ was found to be a major phase on these systems and we conclude these fluxes are not suitable.

In summary, of the total number of flux systems investigated for the LPE growth of SBN, barium-vanadate and potassium-vanadate were found to be the most desirable. Further work on these flux systems is in progress to establish eutectic temperatures, crystallization ranges, and compositional control parameters.

2.3.3 New Tungsten-Bronze Solid-Solution Systems

Strontium-barium-niobate, $Sr_{1-x}Ba_xNb_2O_6$, belongs to the tetragonal tungsten-bronze family and exists over a wide compositional range,[6] i.e., $0.25 \leq X \leq 0.75$. This in itself implies some degree of material parameter control is possible by the ratio of Sr to Ba. A goal of this research is to investigate such a control and to extend its range by additional component substitutions within the tungsten-bronze lattice. Our primary concern for this investigation shall be to determine the temperature stability of the material piezo-elastic constants and to alter them in such a way as to achieve a temperature-compensated piezoelectric material suitable for acoustic signal processing devices.

To synthesize new or modify existing bronze solid solutions based on the $Sr_{1-x}Ba_xNb_2O_6$ system, two modified crystal systems have been investigated using X-ray powder diffraction techniques:

I. $Ba_{1-x}M^+_{x/2}M^{3+}_{x/2}Nb_2O_6$

where M^+ = K, Na or Li

M^{3+} = La, Eu, Gd, or Ho

II. $Ba_{1-x}M^{3+}_xNb_{2-x}M^{4+}_xO_6$

where M^{3+} = La or Gd

M^{4+} = Zr, Sn or Ti

All of the materials are prepared by the solid-state technique using analytical grade materials. After calcining around 800-1000°C for four hours, each batch mixture was ball-milled in acetone for four hours, dried and pressed into disks. The disks were sintered at 1350-1400°C for 10-15 hours in air. Following these procedures, X-ray diffraction techniques were used to identify phase purity and to determine the lattice constants for the different tetragonal tungsten-bronze solid-solutions observed.

For either of the two cases studied above, the end-member, $BaNb_2O_6$, possesses two polymorphic structures. The hexagonal form is stable within a narrow temperature range just below the melting point, 1450°C. The orthorhombic form is stable at lower temperatures. In either structure the short $\bar{c}$ lattice dimension is almost exactly equal to that of the tetragonal bronze type $PbO \cdot X(Nb_2O_5)$ structure, where $1.5 \leq X \leq 3.0$. Although $BaNb_2O_6$ does not belong to the bronze family, the addition of the $M^+ + M^{3+}$ ions for Ba^{2+} or the addition of M^{3+} for Ba^{2+} and M^{4+} for Nb^{5+} introduces the tetragonal tungsten-bronze solid solution.

For the type I substitution, the assemblage can be represented as a pseudo-binary, $BaNb_2O_6$-$M^+M^{3+}Nb_2O_6$. Both of these phases do not belong to the bronze family. $K_{.50}La_{.50}Nb_2O_6$ is isostructural with the paraelectric

phase of $PbTa_2O_6$. The crystalline solid-solubility of $BaNb_2O_6$-$K_{.50}La_{.50}Nb_2O_6$ has been studied and the X-ray diffraction results indicate that the assemblage having composition $0.25 \leq X \leq 0.65$ belongs to the tetragonal tungsten-bronze structure. These phases are well crystallized and can easily be indexed on the tetragonal bronze structure.

The replacement of K^+ by Na^+ in $Ba_{.50}K_{.25}La_{.25}Nb_2O_6$ has been accomplished. Similarly, the substitution of other rare-earths such as Eu^{3+}, Gd^{3+} or Ho^{3+} for La^{3+} in $Ba_{.50}K_{.25}La_{.25}Nb_2O_6$ and $Ba_{.50}Na_{.25}La_{.25}Nb_2O_6$ has been demonstrated. In addition, the synthesis of $Ba_{.50}Li_{.25}M^{3+}_{.25}Nb_2O_6$, where M^{3+} = La, Gd or Ho, produced a mixture of the tungsten-bronze and an unknown phase indicating that partial replacement of K^+ by Li^+ might be possible in the present systems. Such substitutions in the bronze structures are known,[7,8] e.g., $K_3Li_2Nb_5O_{15}$, $K_3Li_2Ta_5O_{15}$.

For the type II system, $Ba_{1-x}La_xNb_{2-x}M^{4+}_xO_6$, where M^{4+} = Zr, Sn or Ti, tetragonal tungsten-bronze solid-solutions have been found. The crystalline solid solubility of $M^{3+} + M^{4+}$ ions is, however, limited as compared to the solid-solubility of $M^+ + M^{3+}$ ions. The tetragonal tungsten-bronze structure exists in the compositional range $0.15 \leq X \leq 0.40$ on the $Ba_{1-x}La_xNb_{2-x}Zr^{4+}_xO_6$. The substitution of Sn^{4+} or Ti^{4+} for Zr^{4+} and Gd^{3+} has been demonstrated. It is expected that the substitution of other rare-earth ions for La^{3+} might be possible in the present system. The substitution of Ti^{4+} as $Ba_6Ti_2Nb_3O_{30}$ is known to exist in this family,[9] however, Zr^{4+} or Sn^{4+} containing tungsten-bronze phases are not known. The incorporation of Zr^{4+} or Sn^{4+} may play a significant role in this structure.

3.0 FUTURE PLANS

3.1 Theoretical Analysis

During the third and fourth quarters, the theoretical modeling to explain why known ferroelectric and ferroelastic materials are temperature-compensated will be continued. The procedure which we will follow is detailed in section 2.2. The objective is to sort by a phenomenological method the prototypic lattice behavior from the ferroelectric and improper ferroelastic instabilities.

3.2 Crystal Growth

During the third and fourth quarters of the present contract, crystalline films of strontium-barium-niobate (SBN) as described in section 2.3.3 will be grown on tungsten-bronze substrates by liquid phase epitaxial techniques. The flux systems described in section 2.3.2 will be used. At this time a limited supply of bulk SBN crystals has been obtained from the University of Tokyo and Honeywell Research Laboratories. We anticipate a larger supply to result from our own bulk crystal growth program now in progress.

3.3 Measurement of Elastic, Piezoelectric and Dielectric Properties

During the third and fourth quarters of the present contract the elastic, piezoelectric and dielectric properties of tungsten-bronze crystals will be measured and compared to known values wherever possible. Particular emphasis will be given to SBN. These measurements will provide the basis for continued theoretical work based on the elastic Gibbs function discussed in section 3.2 above. In addition to the bulk elastic properties, temperature coefficient of delay for surface acoustic waves will be investigated using experimental and theoretical values for the appropriate constants.

4.0 REFERENCES

1. J. C. Toledano, "Theory of the Ferroelastic Transition in Barium Sodim Niobate," Phys. Rev. 12 (3), 943 (1975).

2. R. Roy and W. B. White, "High Temperature Solution and High Pressure Crystal Growth," J. Cryst. Growth 314, 33 (1968).

3. E. J. Staples, R. R. Neurgaonkar, and T. C. Lim, "Temperature Coefficient of SAW Velocity on Epitaxial $Li_{1-x}Na_xNbO_3$ Thin Films," Appl. Phys. Lett. 32 (4), 197 (1978).

4. A. A. Ballman, H. Brown, P. K. Tien, and S. Riva-Sanseverino, "The Growth of $LiNbO_3$ Thin Films by LPE Techniques," J. Cryst. Growth 29, 289 (1975).

5. A. Baudrant, H. Via., and J. Davel, "LPE of $LiNbO_3$ Thin Films for Integrated Optics," Mat. Res. Bull. 10, 1373 (1975).

6. A. A. Ballman and H. Brown, "The Growth and Properties of Strontium Barium Metaniobate, $Sr_{1-x}Ba_xNb_2O_6$, A Tungsten Bronze Ferroelectric," J. Cryst. Growth 1, 311 (1967).

7. T. Fukuda, "Growth and Crystallographic Characteristic of $K_3Li_2Nb_5O_{15}$ Single Crystals," Jap. J. Appl. Phys. 8, 122 (1969).

8. J. Ravez, A. Perron-Simon, and P. Hagenmuller, "Les Phases de Structure, Bronzes de Tungstene Quadratiques," Ann. Chim. t1, 251 (1976).

9. N. C. Stephenson, "The Crystal Structure of the Tetragonal Bronze $Ba_6Ti_2Nb_8O_{30}$," Acta. Cryst. 18, 496 (1965).